*J. Phys. Chem. A* **2005,** *109,* 10759−10769

# Characterizing Hydrogen Bonding and Proton Transfer in 2:1 FH:NH$_3$ and FH:Collidine Complexes through One- and Two-Bond Spin−Spin Coupling Constants across Hydrogen Bonds

**Janet E. Del Bene***

*Department of Chemistry, Youngstown State University, Youngstown, Ohio 44555*

**José Elguero**

*Instituto de Química Médica, CSIC, Juan de la Cierva, 3, E-28006 Madrid, Spain*

*Received: September 25, 2005*

Ab initio equation-of-motion coupled cluster singles and doubles calculations have been carried out on a variety of 2:1 FH:NH$_3$ complexes (F$_b$H$_b$:F$_a$H$_a$:NH$_3$) to investigate the effects of structural changes on one- and two-bond spin−spin coupling constants across F$_a$−H$_a$−N and F$_b$−H$_b$−F$_a$ hydrogen bonds and to provide insight into experimentally measured coupling constants for 2:1 FH:collidine (2:1 FH:2,4,6-trimethylpyridine) complexes. Coupling constants have been computed for 2:1 FH:NH$_3$ equilibrium structures and proton-transferred perpendicular and open structures at 2:1 FH:NH$_3$, FH:pyridine, and FH:collidine geometries. $^{2h}J_{Fa-N}$, $^{1}J_{Fa-Ha}$, and $^{1h}J_{Ha-N}$ exhibit expected dependencies on distances, angles, and the nature of the nitrogen base. In contrast, one- and two-bond coupling constants associated with the F$_b$−H$_b$−F$_a$ hydrogen bond, particularly $^{2h}J_{F_b-F_a}$, vary significantly depending on the F−F distance, the orientation of the hydrogen-bonded pair, and the nature of the complex (HF dimer versus the anion FHF$^-$). The structure of the 2:1 FH:collidine complex proposed on the basis of experimentally measured coupling constants is supported by the computed coupling constants. This study of the structures of open proton-transferred 2:1 FH:NH$_3$, FH:pyridine, and FH:collidine complexes and the coupling constants computed for 2:1 FH:NH$_3$ complexes at these geometries provides insight into the role of the solvent in enhancing proton transfer across both N−H$_a$−F$_a$ and F$_b$−H$_b$−F$_a$ hydrogen bonds.

## Introduction

In a previous paper, we examined spin−spin coupling constants in 1:1 FH:NH$_3$ and FH:pyridine complexes as a function of proton position along the proton-transfer coordinate.[1] The computed one-bond F−H coupling constants ($^{1}J_{F-H}$) for these two complexes are large and positive at equilibrium, but become negative as the proton is transferred and hydrogen-bonded ion-pairs F$^-$:$^+$HNH$_3$ and F$^-$:$^+$Hpyridine are formed. The one-bond H−N coupling constants across the hydrogen bond ($^{1h}J_{H-N}$) are small and positive at equilibrium but become large and negative as the proton is transferred from F to N. Finally, the two-bond F−N coupling constants ($^{2h}J_{F-N}$), where one bond is a hydrogen bond, are always negative and exhibit their maximum absolute values when the hydrogen bonds have quasi-symmetric proton-shared character. The results of that study are consistent with coupling constants for 1:1 FH:collidine (FH:2,4,6-trimethylpyridine) complexes measured experimentally by Limbach et al. as a function of temperature[2,3] and provide further insights into one- and two-bond coupling constants across hydrogen bonds and the sign changes observed for these coupling constants.

Corresponding to the coupling constants $J$ are the reduced coupling constants $K$, given as

$$K_{A-B} \propto J_{A-B}/(\gamma_A)(\gamma_B) \qquad (1)$$

where $\gamma_A$ and $\gamma_B$ are the magnetogyric ratios of nuclei A and B. Since the magnetogyric ratios of $^{19}$F and $^{1}$H are positive while that of $^{15}$N is negative, $^{2h}K_{F-N}$ and $^{1}K_{F-H}$ are positive and $^{1h}K_{H-N}$ is negative for the FH:NH$_3$ and FH:pyridine equilibrium structures. Thus, the signs of these reduced coupling constants are consistent with generalizations made recently concerning the signs of reduced one- and two-bond spin−spin coupling constants across traditional X−H−Y hydrogen bonds. Moreover, $^{1}K_{F-H}$ and $^{1h}K_{H-N}$ change sign as the proton is transferred from F to N.[4−7]

The trimer FH:FH:NH$_3$ was included in a recent study of the effect of a third polar near-neighbor (AH) on one- and two-bond spin−spin coupling constants across the X−H−Y hydrogen bond in trimers AH:XH:YH$_3$, where A and X are $^{19}$F and/or $^{35}$Cl, and Y is either $^{15}$N or $^{31}$P.[8] However, in that study, only X−H, X−Y, and H−Y coupling constants for equilibrium structures were examined. In the present work we expand the study of the F$_b$H$_b$:F$_a$H$_a$:NH$_3$ trimer by (1) investigating changes in F$_a$−H$_a$, H$_a$−N, and F$_a$−N coupling constants along the F$_a$−H$_a$−N proton-transfer coordinate, (2) presenting coupling constants for selected nonequilibrium transition and proton-transferred structures on the trimer potential surface, (3) examining changes in coupling constants involving the F−H−F hydrogen bonds in these complexes, and (4) using coupling constants for 2:1 FH:NH$_3$ complexes computed at 2:1 FH:NH$_3$, 2:1 FH:pyridine, and 2:1 FH:collidine geometries to provide

10.1021/jp055440x CCC: $30.25

further insights into the experimentally measured coupling constants for 2:1 FH:collidine complexes and solvent effects on these coupling constants.

## Methods

The structure of the trimer $F_bH_b$:$F_aH_a$:$NH_3$ was fully optimized at second-order Møller−Plesset theory[9−12] with the 6-31+G(d,p) basis set.[13−16] Vibrational frequencies were computed to confirm that this structure of $C_s$ symmetry is an equilibrium structure on the trimer potential surface. Although this structure has the in-plane N−H bond of $NH_3$ cis to $F_b$, there is only a small barrier of 0.2 kcal/mol to rotation of $NH_3$ about the hydrogen bonding axis. Optimized structures along the $F_a-H_a-N$ proton-transfer coordinate were also obtained. This was done by incrementing the $F_a-H_a$ distance from 0.90 to 2.00 Å in steps of 0.10 Å and, at each distance, optimizing the remaining coordinates always maintaining $C_s$ symmetry. Other structures of interest on the potential surface were also optimized, as well as selected $F_bH_b$:$F_aH_a$:pyridine and $F_bH_b$:$F_aH_a$:collidine complexes.

Coupling constants for $F_bH_b$:$F_aH_a$:$NH_3$ complexes at various geometries have been computed using the ab initio equation-of-motion coupled cluster singles and doubles method (EOM-CCSD) in the CI (configuration interaction)-like approximation[17−20] with the Ahlrichs[21] qzp basis set on F and N, qz2p on the hydrogen-bonded H atoms, and Dunning's cc-pVDZ basis set on other hydrogens.[22,23] The qz2p basis was also placed on the in-plane H of $NH_3$ ($\hat{H}$) when it is cis to the hydrogen bonding region, since this H atom is also a potential proton donor (see structure 1). In the nonrelativistic approximation, the total spin−spin coupling constant is a sum of four contributions: the paramagnetic spin−orbit (PSO), diamagnetic spin−orbit (DSO), Fermi contact (FC), and spin dipole (SD) terms.[24] All terms have been evaluated for all 2:1 FH:$NH_3$ complexes, and FC terms have been computed for selected 2:1 FH:pyridine complexes. All electrons have been correlated in the EOM-CCSD calculations. This level of theory has been shown to give good agreement with available experimental coupling constants.[1,5,25−29] Structure optimizations were done using the Gaussian 03 suite of programs,[30] and coupling constants were evaluated using ACES II.[31] All calculations were performed on the Cray X1 or the Itanium Cluster at the Ohio Supercomputer Center.

## Results and Discussion

**Structure and NMR Properties of the Equilibrium $F_bH_b$:$F_aH_a$:$NH_3$ Complex.** The equilibrium $F_bH_b$:$F_aH_a$:$NH_3$ complex is shown as structure 1. Paramagnetic spin−orbit and Fermi contact terms, total coupling constants for all atoms which lie in the symmetry plane of the equilibrium structure, and corresponding interatomic distances are reported in Table 1. As noted in ref 8, although this complex is stabilized by a traditional $F_a-H_a-N$ hydrogen bond, the proton has moved far enough along the proton-transfer coordinate even in the gas phase to give the hydrogen bond some proton-shared character. This is evident from the length of the $F_a-H_a$ bond, and the small but negative value of $^{1h}J_{Ha-N}$ ($^{1h}K_{Ha-N}$ is positive). The largest coupling constants for atoms which form the $F_a-H_a-N$ hydrogen bond are $^{2h}J_{Fa-N}$ (−70.7 Hz) and $^{1}J_{Fa-Ha}$ (335.8 Hz). Thus, both $^{2h}K_{Fa-N}$ and $^{1}K_{Fa-Ha}$ are large and positive, as expected.[4,5] While the FC term is a good approximation to $^{2h}J_{Fa-N}$, it is not a good approximation to $^{1}J_{Fa-Ha}$ since the PSO term is also significant.

**TABLE 1: Distances and Spin−Spin Coupling Constant Data for the Equilibrium Structure of the $F_bH_b$:$F_aH_a$:$NH_3$ Trimer**

| | distance (Å) | PSO (Hz) | FC (Hz) | *J* (Hz) |
|---|---|---|---|---|
| $N-H_a$ | 1.517 | 0.5 | −2.3 | −2.6 |
| $N-F_a$ | 2.511 | 3.5 | −72.7 | −70.7 |
| $N-H_b$ | 2.952 | 0.1 | 0.1 | 0.1 |
| $N-F_b$ | 3.249 | 0.4 | −2.0 | −1.6 |
| $N-\hat{H}^a$ | 1.016 | −2.3 | −62.0 | −64.6 |
| $H_a-F_a$ | 1.004 | 70.4 | 269.7 | 335.8 |
| $H_a-H_b$ | 2.002 | −2.0 | 0.1 | 0.4 |
| $H_a-F_b$ | 2.689 | −0.5 | −1.5 | −2.4 |
| $F_a-H_b$ | 1.669 | −4.4 | −39.3 | −36.9 |
| $F_a-F_b$ | 2.570 | −73.2 | 25.6 | −32.0 |
| $F_b-H_b$ | 0.946 | 130.7 | 356.7 | 486.1 |
| $F_b-\hat{H}^a$ | 2.703 | 0.9 | 0.1 | 0.2 |

[a] $\hat{H}$ is the in-plane hydrogen atom of $NH_3$ shown for structure 1, which also illustrates the labeling of atoms.

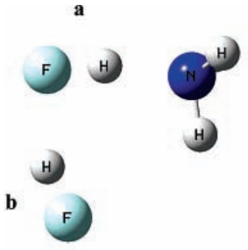

Structure 1

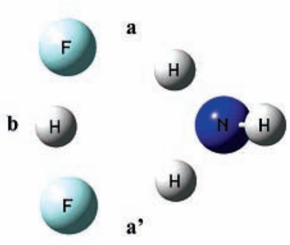

Structure 2

The atoms which form the $F_b-H_b-F_a$ hydrogen bond have positive magnetogyric ratios, which gives the coupling constants (*J*) and the corresponding reduced coupling constants (*K*) the same signs. It was observed previously that both the FC term and $^{2h}J_{F_a-F_b}$ are negative in the equilibrium structure of $(HF)_2$ where the F−F distance is long,[32] and at this distance are exceptions to the generalization that reduced FC terms and reduced two-bond coupling constants across X−H−Y hydrogen bonds are positive when X and Y are the second-period elements $^{13}C$, $^{15}N$, $^{17}O$, and $^{19}F$. It was also noted that the sign and magnitude of the PSO and FC terms and total *J* for F−F coupling are extremely sensitive to the F−F distance and the orientation of the hydrogen-bonded pair. It is interesting to note that the two-bond FC term for $F_a-F_b$ coupling is positive (25.6 Hz) in the trimer but $^{2h}J_{F_a-F_b}$ is negative (−32.0 Hz) due to the large negative value of the PSO term (−73.2 Hz). This situation makes prediction of F−F coupling constants in complexes very difficult. $^{1}J_{F_b-H_b}$ is large and positive, while $^{1h}J_{H_b-F_a}$ has a relatively small negative value, both typical for a traditional hydrogen bond.[5,6] The FC terms and total *J* for $F_a-H_a$ coupling are 269.7 and 335.8 Hz, respectively, while the corresponding values for $F_b-H_b$ are 356.7 and 486.1 Hz, respectively. The FC term and $^{1}J_{F-H}$ in the FH monomer at the equilibrium distance of 0.926 Å are 309.3 and 495.3 Hz, respectively. Thus, while $^{1}J_{F-H}$ has its largest value in the monomer, the FC term does not. Rather, it is the contribution of the PSO term that makes $^{1}J_{F-H}$ greater for the monomer than for $F_b-H_b$ in the equilibrium trimer. Again, this makes it difficult to formulate generalizations concerning one-bond F−H coupling constants in trimers. Nevertheless, the significant decrease of $^{1}J_{F_a-H_a}$ compared to $^{1}J_{F_b-H_b}$ is indicative of the weakening of the $F_a-H_a$ bond due to the increased proton-shared character of the $F_a-H_a-N$ hydrogen bond. The remaining large coupling constant reported in Table 1 is $^{1}J_{N-\hat{H}}$ with a value of −64.6 Hz.

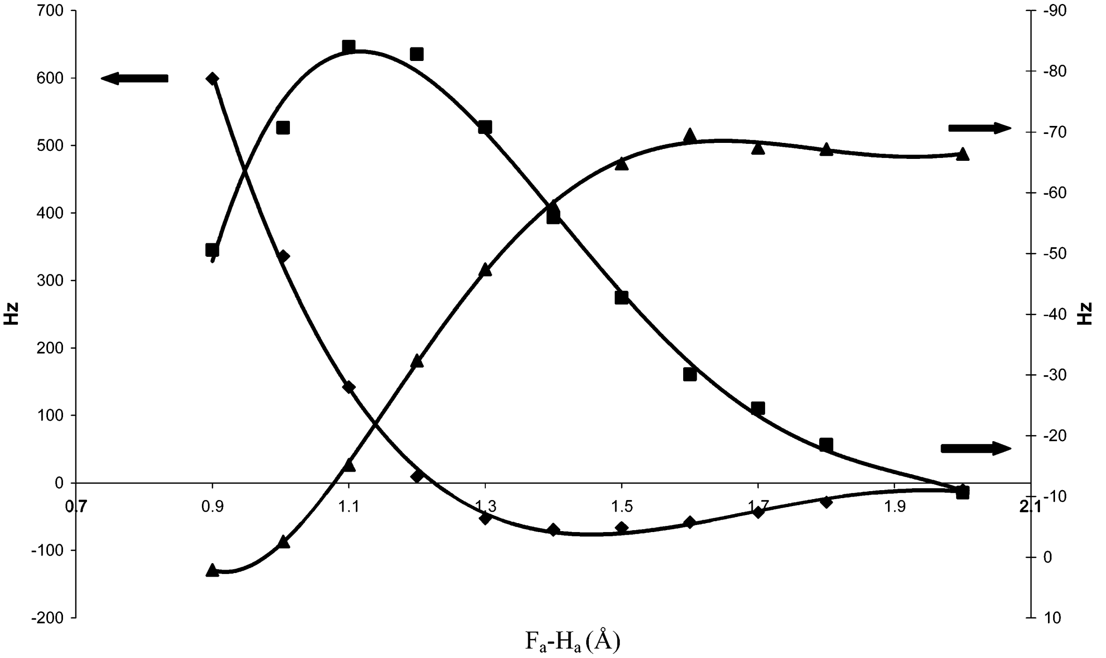

**Figure 1.** Variation of coupling constants $^{1}J_{F_a-H_a}$ (◆), $^{1h}J_{H_a-N}$ (▲), and $^{2h}J_{F_a-N}$ (■) as a function of the F$_a$−H$_a$ distance along the proton-transfer coordinate for the F$_a$−H$_a$−N hydrogen bond. The equilibrium structure is found at an F$_a$−H$_a$ distance of 1.004 Å, and the second point on each curve refers to this structure.

**Structural Changes along the Proton-Transfer Coordinate.** Significant structural changes occur in the trimer as the proton is transferred from F$_a$ to N. At an F$_a$−H$_a$ distance of approximately 1.10 Å, a quasi-symmetric proton-shared hydrogen bond forms. Subsequently, at an F$_a$−H$_a$ distance of about 1.20 Å, H$_a$ transfers to N, and NH$_4^+$ becomes a double proton donor to the FHF$^-$ anion. (The optimized proton-transferred transition structure in which F$_a$ and F$_b$ are equivalent is shown as structure 2. Such a transition structure allows for the interchange of F$_a$ and F$_b$, but not of H$_a$ and H$_b$.) As the F$_a$−H$_a$ distance continues to increase, the F$_b$−H$_b$ bond breaks and a new F$_a$−H$_b$ bond is formed when the F$_a$−H$_a$ distance is about 1.60 Å, and F$_a$−H$_b$ becomes the proton donor to F$_b$. When the F$_a$−H$_a$ distance further increases to 1.70 Å, the in-plane hydrogen atom ($\hat{H}$) of NH$_3$ is transferred to F$_b$, and F$_b$−$\hat{H}$ becomes the proton donor to NH$_3$. The resulting structure is equivalent to that of the original equilibrium structure, with the roles of the two HF molecules interchanged.

In the gas phase, the equilibrium structure of F$_b$H$_b$:F$_a$H$_a$:NH$_3$ has a traditional F$_a$−H$_a$−N hydrogen bond with some proton-shared character. The energy difference between the equilibrium structure 1 and the transition structure 2 is only 8 kcal/mol. Given that experimental measurements of coupling constants are done in solution and that it has been previously demonstrated both experimentally and theoretically that proton transfer can be induced by the solvent,[1−3,33] it is of interest to examine structures and coupling constants for complexes in which proton transfer has occurred, that is, for complexes FHF$^-$:$^+$HNH$_3$. Structures 3 and 4 illustrate two proton-transferred structures of $C_s$ symmetry in which NH$_4^+$ is the proton donor to the anion FHF$^-$. Structure 3 is constrained so that the N, H$_a$, and H$_b$ atoms are collinear, and the N−H$_a$−H$_b$ line bisects the F−F axis and is perpendicular to it. This transition structure also allows for the interchange of the two F atoms but not of H$_a$ and H$_b$. The second proton-transferred structure 4 is one of a series obtained by stretching the F$_a$−H$_a$ distance and then optimizing the complex at that distance. It should be noted that these complexes have the in-plane N−H of NH$_3$ trans to the hydrogen-bond region, and the F$_b$−H$_b$−F$_a$ hydrogen bond is not symmetric. The atoms in the proton-transferred structures have been labeled consistently so that in these and the equilibrium structure 1, F$_a$ is always hydrogen bonded to N through an F$_a$−H$_a$−N hydrogen bond.

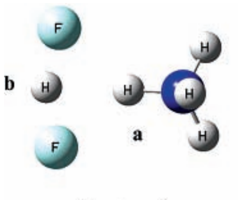

Structure 3

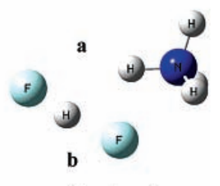

Structure 4

**Changes in Spin−Spin Coupling Constants along the Proton-Transfer Coordinate.** How do spin−spin coupling constants change as the proton H$_a$ is transferred from F$_a$ to N? Figure 1 shows the variation in $^{2h}J_{F_a-N}$, $^{1}J_{F_a-H_a}$, and $^{1h}J_{H_a-N}$ as a function of the F$_a$−H$_a$ distance. The two one-bond coupling constants behave as expected, that is, $^{1}J_{F_a-H_a}$ decreases and becomes negative in the ion-pair complex, while $^{1h}J_{H_a-N}$, which is small but positive at equilibrium, becomes large and negative in the proton-transferred structure. $^{2h}J_{F_a-N}$ exhibits its maximum absolute value at approximately 1.10 Å when a quasi-symmetric proton-shared hydrogen bond is formed. However, as the F$_a$−H$_a$ distance increases, the F$_a$−N coupling constant approaches 0 Hz as F$_a$ and F$_b$ interchange, and F$_a$ is no longer hydrogen bonded to N.

Table 2 presents PSO and FC terms, total couplings constants, and corresponding interatomic distances for the transition structure 2. These may be compared with the coupling constants for the equilibrium trimer reported in Table 1. The two-bond coupling constant $^{2h}J_{Fa-N}$ has a significantly smaller absolute value (−33.1 Hz) in the transition structure than it has in the equilibrium structure (−70.7 Hz). At first this might appear surprising since the F$_a$−N distances in the two structures are similar at 2.513 and 2.511 Å, respectively, and in view of a

**TABLE 2: Distances and Spin−Spin Coupling Constant Data for the Transition Structure of the $F_bH_b$:$F_aH_a$:$NH_3$ Trimer along the Proton-Transfer Coordinate**[a]

| | distance (Å) | PSO (Hz) | FC (Hz) | $J$ (Hz) |
|---|---|---|---|---|
| $N-H_a$ | 1.061 | −0.8 | −67.8 | −68.8 |
| $N-F$ | 2.513 | 2.7 | −35.7 | −33.1 |
| $N-H_b$ | 2.416 | 0.1 | 0.3 | 0.3 |
| $H_a-F_a$ | 1.579 | −9.3 | −53.9 | −59.1 |
| $H_a-H_b$ | 1.894 | −2.9 | 0.1 | 0.3 |
| $H_a-F_{á}$ | 2.475 | −0.2 | −4.4 | −5.1 |
| $F_a-H_b$ | 1.151 | 17.0 | 71.2 | 87.5 |
| $F_a-F_{á}$ | 2.276 | −194.2 | 350.4 | 187.0 |

[a] See structure 2 for labeling of atoms. The two F atoms are equivalent in this structure.

**TABLE 3: Distances and Spin−Spin Coupling Constant Data for a Model Ion-Pair Structure of $F_bH_b$:$F_aH_a$:$NH_3$ in Which the $F-H_b-F$ Hydrogen Bond Is Symmetric**[a]

| | distance (Å) | PSO (Hz) | FC (Hz) | $J$ (Hz) |
|---|---|---|---|---|
| $N-H_a$ | 1.051 | −0.6 | −72.5 | −73.5 |
| $N-F$ | 2.662 | 2.1 | −15.9 | −14.3 |
| $N-H_b$ | 2.633 | 0.1 | 0.0 | 0.0 |
| $H_a-F$ | 1.766 | −4.9 | −20.3 | −20.9 |
| $H_a-H_b$ | 1.582 | −5.8 | 0.2 | 1.3 |
| $F-H_b$ | 1.146 | 18.9 | 59.3 | 77.5 |
| $F-F$ | 2.249 | -270.0 | 312.3 | 73.6 |

[a] See structure 3 for labeling of atoms.

previous observation that at the same F−N distance, two-bond coupling constants across $N-H^+\cdots F$ hydrogen bonds are significantly greater than those across $F-H\cdots N$ hydrogen bonds, since the hydrogen-bonds in the cationic complexes have greater proton-shared character.[34,35] However, the systems for which these observations were made have linear or essentially linear hydrogen bonds. The decreased value of the $N-F_a$ coupling constant in the transition structure 2 may be attributed at least in part to the nonlinearity of the $N-H_a-F_a$ hydrogen bond and may also reflect changes in ground- and excited-state electron densities particularly on N when $NH_4^+$ is a double proton donor for hydrogen bonding.

In structure 2, the $F_a-H_a$ bond is essentially broken as $H_a$ becomes covalently bonded to N. This structural change is accompanied by significant changes in $F_a-H_a$ and $N-H_a$ coupling constants as $F_a$ and N exchange roles as proton donors and acceptors. The one-bond $N-H_a$ coupling constant changes from −2.6 Hz in the equilibrium structure, where it represents a coupling across a hydrogen bond, to −68.8 Hz in the transition structure where it is a one-bond coupling across a covalent bond. Similarly, the $F_a-H_a$ coupling constant of 335.8 Hz for the covalent $F_a-H_a$ bond in the equilibrium structure becomes −59.1 Hz when coupling is across the hydrogen bond in the transition structure.

The remaining coupling constants in structure 2 are those associated with the $FHF^-$ anion in which the hydrogen bond is symmetric but slightly nonlinear. The F−F coupling constant changes significantly from −32.0 Hz in the equilibrium structure to 187.0 Hz in the transition structure due to a significant increase in the FC term and its dominance in the anion. The changes in the two $F-H_b$ coupling constants are consistent with expectations. The $F_b-H_b$ coupling constant associated with the covalent bond in the equilibrium structure remains positive but decreases from 486.1 Hz, and the $F_a-H_b$ coupling constant in the equilibrium structure changes sign and increases. In the transition structure, the two one-bond $F-H_b$ coupling constants are 87.5 Hz. The F−F and $F-H_b$ coupling constants in the transition structure are similar to but smaller than the corresponding coupling constants in the equilibrium MP2/6-31+G(d,p) structure of isolated $FHF^-$ which are 232.1 and 101.3 Hz, respectively, at an F−F distance of 2.299 Å.

**Coupling Constants in Proton-Transferred Structures.** Table 3 presents interatomic distances, PSO and FC terms, and spin−spin coupling constants for an optimized model "perpendicular" ion-pair transition structure 3. It is informative to compare corresponding coupling constants for structures 2 and 3. Most striking are the similarities between $N-H_a$, N−F, $N-H_b$, $H_a-F$, and $H_a-H_b$ coupling constants. For example, ${}^1J_{N-Ha}$ is −73.5 Hz in the perpendicular structure, and −68.8 Hz in the double-donor structure, reflecting similar $N-H_a$ distances of 1.051 and 1.061 Å, respectively. ${}^{2h}J_{N-F}$ is −14.3 Hz in the perpendicular structure 3 and −33.1 Hz in the double-donor structure 2. The smaller value for the perpendicular structure may be attributed to the longer N−F distance and the greater deviation of the $N-H_a-F_a$ hydrogen bond from linearity. Similarly, ${}^{1h}J_{Ha-F}$ is greater for the double-donor structure 2 (−59.1 Hz) than for the perpendicular structure 3 (−20.9 Hz). The $H_a-F$ distance in the double donor structure is 1.579 Å, compared to 1.766 Å in the perpendicular structure. The remaining two coupling constants involving $N-H_b$ and $H_a-H_b$ are small in both complexes.

There are dramatic differences between the F−F coupling constants in the double donor and perpendicular complexes. In the double donor complex, ${}^{2h}J_{F-F}$ is 187.0 Hz, while in the perpendicular complex it is only 73.6 Hz. The difference is due to a more negative PSO term in the perpendicular structure (−270.0 vs −194.2 Hz) and a less positive FC term (312.3 vs 350.4 Hz). The difference in ${}^{2h}J_{F-F}$ certainly would not have been predicted on the basis of the F−F distance, which is shorter in the perpendicular structure (2.249 vs 2.276 Å). The PSO and FC terms for $F-H_b$ coupling in both complexes are positive, with the FC terms dominant. The hydrogen bonds in both complexes are symmetric and slightly nonlinear, and the values of ${}^1J_{F-H_b}$ are similar at 87.5 Hz in the double-donor complex and 77.5 Hz in the perpendicular complex.

Table 4 presents structural data, PSO and FC terms, and total coupling constants for a series of optimized open proton-transferred $NH_4^+$:$FHF^-$ complexes with the in-plane N−H of $NH_4^+$ trans to the hydrogen-bonding region (structure 4). These proton-transferred structures were generated by varying the $F_a-H_a$ distance from 1.50 to 1.90 Å in steps of 0.10 Å, and then optimizing the remaining coordinates at each distance subject to $C_s$ symmetry. As expected, the one-bond $F_a-H_a$ and $N-H_a$ coupling constants in the proton-transferred structures are significantly different from those found in the equilibrium structure as the roles of $F_a$ and N as hydrogen bond donors and acceptors are reversed. In the proton-transferred complexes ${}^{1h}J_{Fa-Ha}$ varies significantly from −61 to −19 Hz as the $F_a-H_a$ distance increases from 1.50 to 1.90 Å. Over this same range of $F_a-H_a$ distances, ${}^1J_{N-Ha}$ increases from −65 to −75 Hz, reflecting a much smaller variation in the $N-H_a$ distance which decreases from 1.086 to 1.032 Å. The two-bond $F_a-N$ coupling constant (${}^{2h}J_{N-F_a}$) decreases from −42 to −12 Hz in this series, due primarily not to the change in the $N-F_a$ distance but to an increased nonlinearity of the $N-H_a-F_a$ hydrogen bond. Thus, even when the in-plane N−H bond of $NH_4^+$ is trans to the hydrogen-bonding region, there is still a strong interaction between $F_b$ and the ammonium hydrogens and a tendency toward cyclization, as evident from the values of the $N-F_a-F_b$ angle.

The F−F and $F-H_b$ coupling constants across the $F_b-H_b-F_a$ hydrogen bonds are significantly different in the open proton-

**TABLE 4: Selected Distances (Å) and Angles (deg) and Spin−Spin Coupling Constant Data (Hz) for Optimized 2:1 FH:NH$_3$ Ion-Pair Complexes as a Function of the $F_a-H_a$ Distance**[a]

Distances and Angles

| $F_a-H_a$ | $N-H_a$ | $N-F_a$ | $N-H_a-F_a$ | $F_b-H_b$ | $F_a-H_b$ | $F_b-F_a$ | $F_b-H_b-F_a$ | $N-F_a-F_b$ |
|---|---|---|---|---|---|---|---|---|
| 1.50 | 1.086 | 2.543 | 159 | 1.024 | 1.332 | 2.328 | 162 | 66 |
| 1.60 | 1.065 | 2.594 | 153 | 1.052 | 1.276 | 2.304 | 163 | 64 |
| 1.70 | 1.050 | 2.634 | 146 | 1.086 | 1.222 | 2.286 | 164 | 62 |
| 1.80 | 1.040 | 2.666 | 138 | 1.131 | 1.166 | 2.277 | 165 | 60 |
| 1.90 | 1.032 | 2.686 | 130 | 1.172 | 1.125 | 2.278 | 165 | 59 |

Coupling Constants

| $F_a-H_a$ | $^{1h}J_{F_a-H_a}$ | $^{1}J_{N-H_a}$ | $^{2h}J_{N-F_a}$ | $^{1}J_{F_b-Hb}$ | $^{1h}J_{H_b-F_a}$ | $^{2h}J_{F_b-F_a}$ |
|---|---|---|---|---|---|---|
| 1.50 | −60.5 | −64.9 | −41.6 | 314.0 | −42.0 | 94.5 |
| 1.60 | −49.1 | −69.6 | −30.7 | 252.4 | −22.2 | 129.7 |
| 1.70 | −37.3 | −72.5 | −22.4 | 183.9 | 11.7 | 160.3 |
| 1.80 | −27.0 | −74.1 | −16.2 | 110.7 | 64.6 | 177.3 |
| 1.90 | −18.8 | −75.1 | −11.9 | 57.1 | 119.3 | 175.6 |

PSO Terms

| $F_a-H_a$ | $F_a-H_a$ | $N-H_a$ | $N-F_a$ | $F_b-H_b$ | $F_a-H_b$ | $F_b-F_a$ |
|---|---|---|---|---|---|---|
| 1.50 | −9.3 | −0.4 | 3.3 | 60.6 | −1.7 | −179.5 |
| 1.60 | −8.4 | −0.6 | 2.8 | 47.0 | 1.5 | −195.4 |
| 1.70 | −7.0 | −0.8 | 2.3 | 34.0 | 6.7 | −207.8 |
| 1.80 | −5.5 | −1.0 | 1.9 | 21.8 | 14.7 | −215.9 |
| 1.90 | −4.2 | −1.1 | 1.5 | 13.6 | 23.4 | −219.0 |

Fermi Contact Terms

| $F_a-H_a$ | $F_a-H_a$ | $N-H_a$ | $N-F_a$ | $F_b-H_b$ | $F_a-H_b$ | $F_b-F_a$ |
|---|---|---|---|---|---|---|
| 1.50 | −55.0 | −64.1 | −44.0 | 257.4 | −45.3 | 246.2 |
| 1.60 | −44.7 | −68.6 | −33.0 | 209.0 | −27.4 | 295.6 |
| 1.70 | −34.1 | −71.4 | −24.6 | 152.6 | 3.0 | 337.5 |
| 1.80 | −24.8 | −72.9 | −18.2 | 90.2 | 49.8 | 362.2 |
| 1.90 | −17.3 | −73.8 | −13.7 | 43.2 | 97.3 | 364.0 |

[a] See structure 4 for labeling of atoms.

transferred structures compared to the equilibrium structure. The most dramatic difference is found for $^{2h}J_{F_a-F_b}$. In the equilibrium structure 1, the PSO term (−73.2 Hz) dominates the FC term (25.6 Hz), and $^{2h}J_{F_a-F_b}$ is −32.0 Hz. In the proton-transferred structures 4, the FC term is large and positive (between 246 and 364 Hz) while the PSO term is large and negative (between −180 and −219 Hz). Since the FC term dominates, $^{2h}J_{F_a-F_b}$ is large and positive, ranging from 95 to 176 Hz. Thus, the F−F coupling constant in the equilibrium structure more closely resembles the F−F coupling constant in $(HF)_2$, whereas the F−F coupling constants in the open ion-pair structures more closely resemble that of the anion $F-H-F^-$. The one-bond $F_b-H_b$ and $F_a-H_b$ coupling constants vary dramatically depending on the corresponding distances, with $^{1h}J_{H_b-F_a}$ even changing sign as the $F_a-H_a$ distance increases and the proton-shared character of the $F_b-H_b-F_a$ hydrogen bond increases.

**Relating Computed 2:1 FH:NH$_3$ Coupling Constants to 2:1 FH:Collidine Experimental Data.** One of the motivating factors behind this study was the paper by Limbach et al. on coupling constants in 2:1 FH:collidine complexes.[7] The preferred theoretical approach to this problem would be to compute coupling constants for 2:1 FH:collidine complexes, but this is not feasible because of the number of basis functions and the amount of CPU time required. The next option would be to compute coupling constants for 2:1 FH:pyridine complexes. Unfortunately, this is not computationally feasible for most of the complexes of interest. However, it is possible to evaluate the Fermi contact term in 1:1 and 2:1 perpendicular proton-transferred FH:pyridine complexes, and this has been done. Thus, insights into the properties of 2:1 FH:collidine complexes from ab initio theoretical studies must come at this time from a systematic study of the structures of 2:1 FH:NH$_3$, FH:pyridine, and FH:collidine complexes, computed coupling constants for FH:NH$_3$ complexes with geometries in the hydrogen-bonding region taken from the complexes with the three different nitrogen bases, and comparison with experimental data. It is therefore imperative that the following two questions be addressed.

(1) What effects do geometry differences between corresponding 2:1 FH:NH$_3$ and FH:collidine complexes have on coupling constants?

(2) What are the effects on coupling constants when NH$_3$ instead of collidine is used as the base?

**Coupling Constants and Geometry Differences.** Table 5 reports interatomic distances for optimized equilibrium structures with $F_a-H_a\cdots N$ hydrogen bonds and perpendicular proton-transferred structures for 2:1 FH:NH$_3$, 2:1 FH:pyridine, and 2:1 FH:collidine complexes. Equilibrium 2:1 FH:pyridine and 2:1 FH:collidine complexes are illustrated as structures 5 and 6, respectively. The coupling constants reported in Table 5 were obtained from calculations on 2:1 FH:NH$_3$ complexes with the geometries in the hydrogen-bonding regions taken from corresponding 2:1 FH:NH$_3$, 2:1 FH:pyridine, and 2:1 FH:collidine complexes. The first set of data in Table 5 refers to optimized geometries in which $F_a-H_a$ is the proton donor to N. In these, a pattern of changes in distances and corresponding coupling constants is readily observed. As the nitrogen base becomes stronger in going from NH$_3$ to pyridine to collidine, the $N-F_a$ distance decreases, and the absolute value of $^{2h}J_{F_a-N}$ increases. Moreover, as the $N-F_a$ distance decreases, the $F_a-H_a$ distance increases, with the result that $^{1}J_{F_a-H_a}$ decreases dramatically from 355.3 Hz at the geometry of the 2:1 FH:NH$_3$ complex to 271.9 and 254.3 Hz in the two complexes with geometries taken from the “trans” and “cis” 2:1 FH:collidine complexes. (Here, “trans” and “cis” refer to the orientation of the in-plane C−H bonds of

**TABLE 5: Selected Coupling Constants for 2:1 FH:NH$_3$ Complexes at Optimized Geometries for Corresponding 2:1 FH:Pyridine and FH:Collidine Complexes**

Optimized Structures with Traditional Hydrogen Bonds[a]

| | $F_a-N$ | | $F_a-H_a$ | | $H_a-N$ | |
|---|---|---|---|---|---|---|
| | *R* (Å) | *J* (Hz) | *R* (Å) | *J* (Hz) | *R* (Å) | *J* (Hz) |
| NH$_3$[b] | 2.525 | −71.6 | 1.000 | 355.3 | 1.526 | −2.2 |
| pyridine[c] | 2.483 | −78.7 | 1.019 | 302.3 | 1.468 | −4.9 |
| collidine[d] | 2.465 | −86.1 | 1.038 | 271.9 | 1.428 | −7.4 |
| collidine[e] | 2.457 | −88.8 | 1.046 | 254.3 | 1.411 | −8.8 |

| | $F_a-F_b$ | | $F_b-H_b$ | | $H_b-F_a$ | |
|---|---|---|---|---|---|---|
| | *R* (Å) | *J* (Hz) | *R* (Å) | *J* (Hz) | *R* (Å) | *J* (Hz) |
| NH$_3$[b] | 2.588 | −16.6 | 0.944 | 488.3 | 1.656 | −42.8 |
| pyridine[c] | 2.552 | −18.8 | 0.949 | 478.2 | 1.626 | −44.2 |
| collidine[d] | 2.552 | +1.4 | 0.949 | 481.0 | 1.607 | −51.3 |
| collidine[e] | 2.538 | +6.4 | 0.950 | 480.1 | 1.594 | −53.3 |

Perpendicular Proton-Transferred Structures

| | $F-N$ | | $F-H_a$ | | $H_a-N$ | |
|---|---|---|---|---|---|---|
| | *R* (Å) | *J* (Hz) | *R* (Å) | *J* (Hz) | *R* (Å) | *J* (Hz) |
| NH$_3$[b] | 2.662 | −14.3 | 1.766 | −20.9 | 1.051 | −73.5 |
| pyridine[c] | 2.674 | −13.1 | 1.784 | −19.0 | 1.043 | −74.1 |
| collidine[d] | 2.834 | −7.8 | 1.924 | −10.1 | 1.041 | −74.7 |
| collidine[e] | 2.957 | −5.3 | 2.036 | −5.6 | 1.038 | −75.0 |

| | $F-F$ | | $F-H_b$ | |
|---|---|---|---|---|
| | *R* (Å) | *J* (Hz) | *R* (Å) | *J* (Hz) |
| NH$_3$[b] | 2.249 | 73.6 | 1.146 | 77.5 |
| pyridine[c] | 2.256 | 70.3 | 1.146 | 77.2 |
| collidine[d] | 2.252 | 109.1 | 1.139 | 86.1 |
| collidine[e] | 2.255 | 121.5 | 1.137 | 89.8 |

[a] For all of these model calculations, the in-plane N−H bond of NH$_3$ is trans to the hydrogen-bonding region. [b] Distances from the optimized 2:1 FH:NH$_3$ complex with the in-plane N−H bond of NH$_3$ trans to the hydrogen-bonding region. This is not the equilibrium structure of this complex. [c] Distances from the optimized 2:1 FH:pyridine complex. Structure 5 is the equilibrium structure, and structure 7 is the perpendicular proton-transferred structure. [d] Distances from the optimized 2:1 FH:collidine complex in which the in-plane C−H bond of the methyl groups in the 2 and 6 positions are trans to the hydrogen bonding region. Structure 6 is the equilibrium structure and structure 8 is the perpendicular proton-transferred structure. [e] Distances from the optimized 2:1 FH:collidine complex in which the in-plane C−H bond of the methyl groups in the 2 and 6 positions are cis to the hydrogen-bonding region.

the methyl groups in the 2 and 6 positions relative to the hydrogen-bonding region.) Similarly, as the H$_a$−N distance decreases, the absolute value of $^{1h}J_{H_a-N}$ increases in the series.

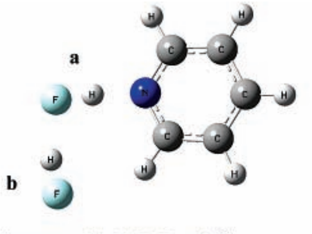

Structure 5 (<N-F$_a$-F$_b$ = 91°)

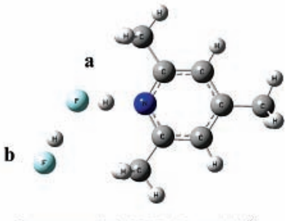

Structure 6 (<N-F$_a$-F$_b$ = 115°)

While a pattern of geometry dependence of coupling constants is readily recognizable for coupling across the $F_a-H_a\cdots N$ hydrogen bond, this is not the case for F−F coupling across the $F_b-H_b\cdots F_a$ hydrogen bond. This is not unexpected, for in these complexes the HF dimer is the proton donor to the nitrogen bases, and F−F coupling constants in this dimer are extremely sensitive to distance and the orientation of the hydrogen-bonded pair.[32] Thus, the F−F coupling constant is −16.6 Hz at the 2:1 FH:NH$_3$ geometry, −18.8 Hz at the 2:1 FH:pyridine geometry, but +1.4 and +6.4 Hz at the trans and cis geometries, respectively, of the 2:1 FH:collidine complexes. The difference between the F−F coupling constants at the 2:1 FH:pyridine versus the trans 2:1 FH:collidine geometry is due primarily to an increase in the Fermi contact term, from 40.9 to 58.5 Hz. Since the F−F distances in these two complexes are essentially identical, this difference must be related to the orientation of the HF dimer, as described by the $F_b-F_a-H_a$ angle. This angle is 91° in structure 5 and 115° in structure 6, indicating that the complex with collidine has a more open structure in the hydrogen-bonding region.

The one-bond coupling constants do not exhibit any unusual geometry dependence in these complexes in which $F_b-H_b$ is the proton donor to F$_a$. $^{1}J_{F_b-H_b}$ is 488.3 Hz at the 2:1 FH:NH$_3$ geometry and decreases as the $F_b-H_b$ distance increases slightly in the 2:1 FH:pyridine complex. The $F_b-H_b$ distances are essentially identical at the pyridine and collidine geometries, and the coupling constants for 2:1 FH:NH$_3$ complexes at these geometries differ by only 3 Hz. Similarly, $^{1h}J_{H_b-F_a}$ is negative in all complexes, and its absolute value increases as the $H_b-F_a$ distance decreases.

Table 5 also presents coupling constant data for 2:1 optimized perpendicular proton-transferred complexes computed for 2:1 FH:NH$_3$ complexes at geometries taken from the corresponding 2:1 FH:NH$_3$ (structure 3), 2:1 FH:pyridine (structure 7), and 2:1 FH:collidine (structure 8) complexes. The $F_a-H_a-N$ hydrogen bonds in these complexes deviate significantly from linearity and the $F-H_a$ distances are long, with the result that all F−N coupling constants are significantly reduced relative to the equilibrium complexes. As the F−N and $F-H_a$ distances increase, F−N and $F-H_a$ coupling constants decrease in absolute value. These two coupling constants are similar at the 2:1 FH:NH$_3$ and FH:pyridine geometries but are reduced at the 2:1 FH:collidine trans and cis geometries, owing to much longer F−N and $F-H_a$ distances. The $N-H_a$ distance is similar at all four geometries, and $H_a-N$ coupling constants differ by only 2.5 Hz.

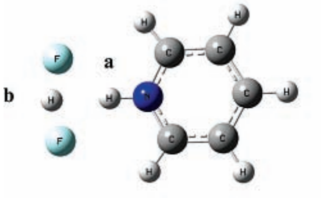

Structure 7

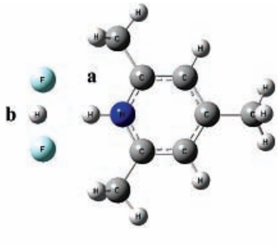

Structure 8

Once again it is the F−F coupling constants that exhibit unusual behavior. Although F−F coupling constants in FHF$^-$ are extremely sensitive to distance, the small variations in the F−F distances cannot be primarily responsible for the large differences observed for these coupling constants, particularly at the 2:1 FH:pyridine and 2:1 FH:collidine cis geometries, where the F−F distances are essentially identical but the F−F coupling constants are 70.3 and 121.5 Hz, respectively. What is different about the structures of these two complexes? The answer lies in the three structural parameters that are reported in Table 6. These show that the distance between the FHF$^-$ anion and the $N-H_a$ donor (as measured by the distance between the N atom and X, the midpoint of the F−F axis) is significantly greater in the complexes with collidine compared to NH$_3$ and

**TABLE 6: Selected Distances (Å) and Angles (deg) for Perpendicular Proton-Transferred Complexes with Symmetric F−H$_b$−F Hydrogen Bonds**

| complex | *R* (N−X)[a] | *R* (N−H$_b$) | H$_b$−F−F |
|---|---|---|---|
| 2:1 FH:NH$_3$ | 2.413 | 2.633 | 11.1 |
| 2:1 FH:pyridine | 2.424 | 2.628 | 10.2 |
| 2:1 FH:collidine (trans) | 2.600 | 2.771 | 8.6 |
| 2:1 FH:collidine (cis) | 2.733 | 2.876 | 7.2 |

[a] X is the midpoint of the F−F line.

pyridine and that H$_b$ is closer to the F−F line at the collidine geometries. This means that the anion F−H$_b$−F$^-$ is farther removed from the N−H$_a$ donor and that the F−H$_b$−F hydrogen bond deviates from linearity to a lesser extent at the collidine geometries. As a result, the F−F coupling constants are greater. The F−H$_b$ coupling constants are also greater at the 2:1 FH:collidine geometries (86.1 and 89.8 Hz at the trans and cis geometries, respectively) compared with the FH:NH$_3$ and FH:pyridine (77.5 and 77.2 Hz) geometries. The larger values at the collidine geometries correlate with the shorter F−H$_b$ distances.

Since proton-transferred structures are not minima on the potential surfaces in the gas phase, it is not possible to fully optimize such 2:1 FH:NH$_3$ (structure 4), 2:1 FH:pyridine (structure 9), and 2:1 FH:collidine (structure10) complexes. However, these can be obtained by imposing some constraint, such as requiring that the F$_a$−H$_a$ distance be relatively long as is the case in ion-pair complexes.[36] This has been done systematically by varying the F$_a$−H$_a$ distance and at each distance optimizing the remaining coordinates subject to $C_s$ symmetry. Selected interatomic distances and angles for proton-transferred 2:1 FH:pyridine and 2:1 FH:collidine complexes at a series of F$_a$−H$_a$ distances are reported in Table 7, along with the coupling constants computed for 2:1 FH:NH$_3$ complexes at the geometries of the pyridine and collidine complexes in the hydrogen bonding regions. Corresponding data for the 2:1 FH:NH$_3$ complexes are given in Table 4. As evident from Tables 4 and 7, $^{1}J_{\mathrm{N-H_a}}$, $^{1h}J_{\mathrm{H_a-F_a}}$, and $^{2h}J_{\mathrm{N-F_a}}$ exhibit similar behavior with little dependence on whether the optimized geometries are taken from 2:1 FH:NH$_3$, 2:1 FH:pyridine, or 2:1 FH:collidine complexes. At all geometries, as the F$_a$−H$_a$ distance increases $^{1h}J_{\mathrm{H_a-F_a}}$ is negative and always decreases in absolute value. These negative values indicate that the N−H$_a$−F$_a$ hydrogen bonds do not have significant proton-shared character. Moreover, as the F$_a$−H$_a$ distance increases, the F$_a$−N distance increases and the N−H$_a$ distance decreases, and these distance changes correlate with the decreasing absolute values of $^{2h}J_{\mathrm{N-F_a}}$ and increasing absolute values of $^{1}J_{\mathrm{N-H_a}}$.

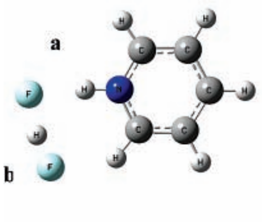

Structure 9

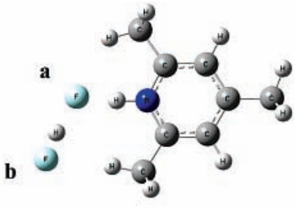

Structure 10

In contrast, there are significant differences among coupling constants which involve the atoms that form the F$_b$−H$_b$−F$_a$ hydrogen bond due to differences in the geometries in the hydrogen-bonding regions of 2:1 FH:NH$_3$, 2:1 FH:pyridine, and 2:1 FH:collidine complexes. A comparison of the behavior of $^{2h}J_{\mathrm{F_b-F_a}}$, $^{1}J_{\mathrm{F_b-H_b}}$, and $^{1h}J_{\mathrm{H_b-F_a}}$ for complexes at 2:1 FH:NH$_3$, FH:pyridine, and FH:collidine geometries as the F$_a$−H$_a$ distance increases from 1.60 to 1.80 Å illustrates this variation quite well. When these coupling constants are computed at 2:1 FH:NH$_3$ geometries in this distance range, $^{2h}J_{\mathrm{F_b-F_a}}$ increases from 130 to 177 Hz, $^{1h}J_{\mathrm{H_b-F_a}}$ changes sign, and $^{1}J_{\mathrm{F_b-H_b}}$ decreases from 252 to 111 Hz. At the 2:1 FH:pyridine geometries over the same range of F$_a$−H$_a$ distances, $^{2h}J_{\mathrm{F_b-F_a}}$ varies by 14 Hz, $^{1h}J_{\mathrm{H_b-F_a}}$ also changes sign, and $^{1}J_{\mathrm{F_b-H_b}}$ decreases from 286 to 154 Hz. Over the same range of distances at the 2:1 FH:collidine geometries, $^{2h}J_{\mathrm{F_b-F_a}}$ varies by only 3 Hz, $^{1h}J_{\mathrm{H_b-F_a}}$ decreases from −53 to −36 Hz but does not change sign, and $^{1}J_{\mathrm{F_b-H_b}}$ decreases from 353 to 292 Hz. The geometry dependence is not simply a distance dependence but most probably reflects the change in the orientation of the F−H$_b$−F$^-$ anion relative to the nitrogen base, as can be seen by comparing structures 4, 9, and 10, and values of the N−F$_a$−F$_b$ angle given in Tables 4 and 7. In the 2:1 FH:NH$_3$ complexes the N−F$_a$−F$_b$ angle is approximately 60° when the F$_a$−H$_a$ distance ranges from 1.60 to 1.80 Å. This acute angle signals cyclization and favors interaction between F$_b$ and the two NH$_4^+$ hydrogens that lie above and below the hydrogen bonding plane. As a result, H$_b$ moves toward F$_a$ and the F$_b$−H$_b$−F$_a$ hydrogen bond acquires the highest degree of proton-shared character among the proton-transferred 2:1 complexes of FH with the nitrogen bases. The values of the N−F$_a$−F$_b$ angle for the 2:1 FH:pyridine complexes also suggest that F$_b$ interacts favorably with the pyridine ring, and this interaction also leads to increased proton-shared character of the F$_b$-H$_b$−F$_a$ hydrogen bond. In contrast, the N−F$_a$−F$_b$ angle is much greater at the 2:1 FH:collidine geometries, and the F$_b$−H$_b$−F$_a$ hydrogen bond appears to have little proton-shared character in the gas phase. Knowing how these coupling constants vary will be important when comparing computed coupling constants for 2:1 complexes with those measured experimentally for 2:1 FH:collidine complexes in Freon solutions.

**Dependence of Coupling Constants on the Nature of the N Atom.** Another informative comparison can be made between 1:1 and 2:1 FH:NH$_3$ and FH:pyridine complexes. Unfortunately, EOM-CCSD calculations of total coupling constants for FH:pyridine complexes are not feasible. However, Fermi contact terms can be evaluated for 1:1 FH:pyridine complexes and 2:1 FH:pyridine perpendicular proton-tranferred complexes. F−N, F−H, and H−N coupling constants for 1:1 FH:NH$_3$ and 1:1 FH:pyridine complexes as a function of the F−H distance are plotted in Figure 2, and data for these complexes at an F−H distance of 1.50 Å are given in Table 8. It is apparent from Figure 2 and Table 8 that Fermi contact terms for F−H coupling are essentially independent of the nature of the nitrogen base. The F−N Fermi contact term is always greater for FH:pyridine than FH:NH$_3$ at the same F−H distance, but the F−N distance is also slightly shorter and the behavior of both along the proton-transfer coordinate is similar. The difference between them is greatest for a quasi-symmetric proton-shared hydrogen bond (at an F−H distance of approximately 1.2 Å), but as proton transfer occurs, the difference decreases. In contrast, the H−N coupling constants are sensitive to the nature of the N atom, as evident from the FC terms which have values of −54.8 and −73.9 Hz in the FH:NH$_3$ and FH:pyridine complexes, respectively, when the F−H distance is 1.50 Å. This difference is also apparent when the computed values of $^{1}J_{\mathrm{N-H}}$ for the cations ammonium (−75 Hz) and pyridinium (−92 Hz) are compared. However, the Fermi contact terms for coupling in these two complexes exhibit the same qualitative behavior along the proton-transfer coordinate.

How do the Fermi contact terms for the optimized 2:1 FH:pyridine perpendicular structure and a 2:1 FH:NH$_3$ perpendicular

**TABLE 7: Selected Distances (Å) and Angles (deg) and Spin−Spin Coupling Constants (Hz) for 2:1 FH:NH$_3$ Ion-Pair Complexes at Optimized 2:1 FH:Pyridine and 2:1 FH:Collidine Geometries as a Function of the F$_a$−H$_a$ Distance**

2:1 FH:Pyridine[a]

| | Distances and Angles | | | | | | | |
|---|---|---|---|---|---|---|---|---|
| F$_a$−H$_a$ | N−H$_a$ | N−F$_a$ | N−H$_a$−F$_a$ | F$_b$−H$_b$ | F$_a$−H$_b$ | F$_b$−F$_a$ | F$_b$−H$_b$−F$_a$ | N−F$_a$−F$_b$ |
| 1.60 | 1.062 | 2.658 | 173 | 1.038 | 1.296 | 2.322 | 168 | 79 |
| 1.70 | 1.048 | 2.746 | 175 | 1.063 | 1.252 | 2.302 | 168 | 75 |
| 1.80 | 1.037 | 2.834 | 174 | 1.104 | 1.194 | 2.280 | 166 | 67 |

| | Coupling Constants | | | | | |
|---|---|---|---|---|---|---|
| F$_a$−H$_a$ | $^{1h}J_{F_a-H_a}$ | $^{1}J_{N-H_a}$ | $^{2h}J_{N-F_a}$ | $^{1}J_{F_b-H_b}$ | $^{1h}J_{H_b-F_a}$ | $^{2h}J_{F_b-F_a}$ |
| 1.60 | −45.4 | −69.2 | −32.8 | 285.6 | −37.8 | 108.4 |
| 1.70 | −33.0 | −72.7 | −23.2 | 233.1 | −17.4 | 122.3 |
| 1.80 | −21.2 | −76.0 | −14.2 | 153.8 | 24.8 | 116.3 |

2:1 FH:Collidine[b]

| | Distances and Angles | | | | | | | |
|---|---|---|---|---|---|---|---|---|
| F$_a$−H$_a$ | N−H$_a$ | N−F$_a$ | N−H$_a$−F$_a$ | F$_b$−H$_b$ | F$_a$−H$_b$ | F$_b$−F$_a$ | F$_b$−H$_b$−F$_a$ | N−F$_a$−F$_b$ |
| 1.50 | 1.079 | 2.573 | 172 | 0.998 | 1.379 | 2.370 | 171 | 106 |
| 1.60 | 1.060 | 2.649 | 169 | 1.009 | 1.350 | 2.351 | 171 | 101 |
| 1.70 | 1.047 | 2.727 | 166 | 1.021 | 1.322 | 2.335 | 170 | 95 |
| 1.80 | 1.039 | 2.804 | 161 | 1.035 | 1.294 | 2.320 | 170 | 91 |
| 1.90 | 1.034 | 2.877 | 156 | 1.056 | 1.254 | 2.299 | 169 | 89 |

| | Coupling Constants | | | | | |
|---|---|---|---|---|---|---|
| F$_a$−H$_a$ | $^{1h}J_{F_a-H_a}$ | $^{1}J_{N-H_a}$ | $^{2h}J_{N-F_a}$ | $^{1}J_{F_b-H_b}$ | $^{1h}J_{H_b-F_a}$ | $^{2h}J_{F_b-F_a}$ |
| 1.50 | −57.2 | −63.8 | −49.5 | 379.5 | −58.1 | 98.7 |
| 1.60 | −46.4 | −68.5 | −37.4 | 352.9 | −53.1 | 102.8 |
| 1.70 | −34.7 | −71.8 | −27.8 | 324.4 | −46.1 | 102.4 |
| 1.80 | −24.4 | −74.3 | −20.2 | 291.5 | −36.1 | 99.5 |
| 1.90 | −15.8 | −76.1 | −14.0 | 243.5 | −17.2 | 101.9 |
| ref 7 | −75 | −86 | ? | 280 | <10 | 155 |

[a] See structure 9 for the labeling of atoms in complexes with pyridine. [b] See structure 10 for the labeling of atoms in complexes with collidine.

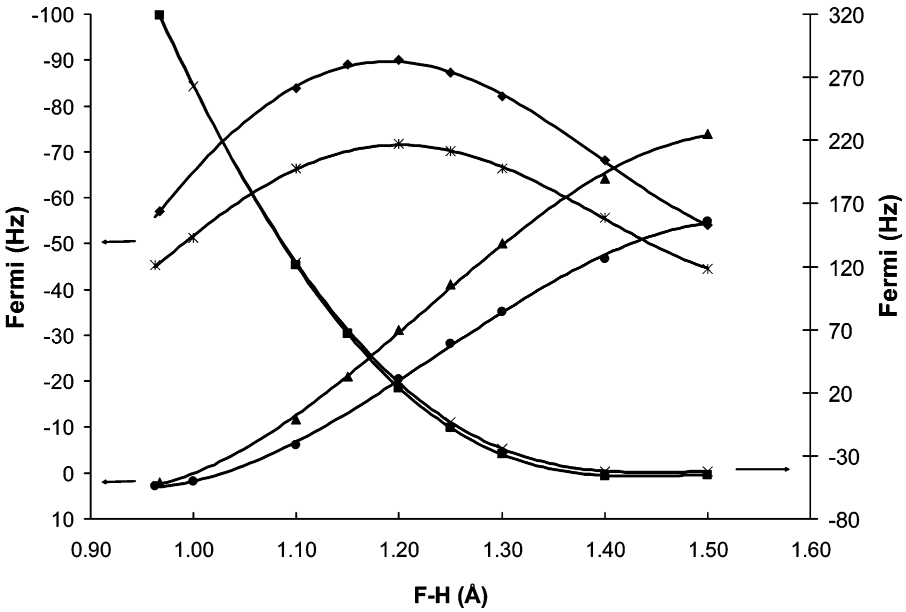

**Figure 2.** Variation of the FC terms for coupling across the F−H−N hydrogen bonds in 1:1 FH:NH$_3$ and FH:pyridine complexes as a function of the F−H distance. The curves are in pairs, with the upper curve corresponding to coupling in FH:pyridine. The F−N and H−N curves are read on the left axis. The F−N curves show a maximum for a proton-shared quasi-symmetric hydrogen bond, while the H−N coupling constant curves show a dependence on the nature of N as proton transfer occurs. The curves for F−H coupling are read on the right axis and are essentially independent of the nature of N.

complex at the FH:pyridine geometry compare? Data for these two complexes are also reported in Table 8. The most striking observation is the similarly between corresponding FC terms for these two 2:1 proton-transferred complexes. The F−N and F−H$_a$ FC terms are both relatively small and negative with values of −14.7 and −13.6 Hz and −18.5 and −18.8 Hz, respectively. The N−H$_a$ coupling constant does show a dependence on the nature of the N atom, with a larger absolute value in the 2:1 FH:pyridine complex (−93.2 Hz) versus the 2:1 FH:NH$_3$ complex (−73.1 Hz). This is as expected and in agreement

**TABLE 8: Comparison of Fermi Contact Terms (Hz) for 1:1 and 2:1 FH:NH$_3$ and FH:Pyridine Complexes Computed at the Proton-Transferred Geometries of the Pyridine Complexes**

| 1:1 complexes[a] | F−N | F−H | N−H |
|---|---|---|---|
| FH:NH$_3$ | −44.6 | −42.5 | −54.8 |
| FH:pyridine | −54.1 | −45.3 | −73.9 |

| 2:1 complexes[b] | F−N | F−H$_a$ | N−H$_a$ | F−F | F−H$_b$ |
|---|---|---|---|---|---|
| FH:NH$_3$ | −14.7 | −18.5 | −73.1 | 305.9 | 58.9 |
| FH:pyridine | −13.6 | −18.8 | −93.2 | 339.1 | 63.0 |

[a] Values of the Fermi contact terms from ref 1 for the complexes in which the F−H distance was constrained at 1.50 Å. The hydrogen bonds are linear, and the F−N distances are 2.614 and 2.605 Å in FH:NH$_3$ and FH:pyridine, respectively. [b] Fermi contact terms at the geometry of the FH:pyridine complex shown as structure 7.

with experimental data for N−H coupling constants.[37] Even the Fermi contact terms for F−F and F−H coupling are similar, although in the presence of pyridine, both the F−F and F−H$_b$ coupling constants are greater than they are when NH$_3$ is the base. Thus, using NH$_3$ instead of pyridine (or collidine) does not dramatically change FC terms, but it does have an effect on the magnitude of Fermi contact terms for N−H$_a$, F−F, and F−H$_b$ coupling.

**Interpreting the Experimental Data from Computed Structures and Coupling Constants.** Although the changes in coupling constants due to structural changes in the 2:1 FH:NH$_3$ complexes are of interest in themselves, one of the motivating factors for this study was to determine if structures and coupling constants for these complexes could be useful for gaining further insight into the structure of the 2:1 FH:collidine complex that exists in solution and gives rise to the coupling constants measured experimentally. We agree with the observation made in ref 7 that at low temperature in solution, proton transfer from F$_a$ to N occurs. (In previous studies of 1:1 FH:collidine complexes,[1−3] it was shown that the solvent converts a traditional F−H···N hydrogen bond into a proton-shared F···H···N hydrogen bond at low temperature. Thus, it should be expected that the 2:1 FH:collidine complex, which has a greater degree of proton-shared character even in the gas phase, should become an ion-pair structure at low temperature.) Our results also agree with ref 7 that the structure which most probably exists in solution is an open proton-transferred structure (structure 10). The optimized open proton-transferred structures with F$_a$−H$_a$ distances between 1.80 and 1.60 Å are about 2−6 kcal/mol more stable than the optimized perpendicular structure 8. These values are in agreement with Limbach's estimate that the barrier to the interchange of F$_a$ and F$_b$ in solution is about 5 kcal/mol.[7] What now remains is to see how well the computed coupling constants for these open proton-transferred structures match experimental values.

Experimental spin−spin coupling constants for N−H$_a$−F$_a$ and F$_b$−H$_b$−F$_a$ hydrogen bonds can be compared with computed coupling constants for 2:1 FH:NH$_3$ complexes at proton-transferred 2:1 FH:NH$_3$, 2:1 FH:pyridine, and 2:1 FH:collidine geometries using the data of Tables 4 and 7. Independent of whether the optimized complex contains NH$_3$, pyridine, or collidine as the base, the best agreement between the experimental and computed values of $^{1h}J_{H_a-F_a}$ is found at short F$_a$−H$_a$ distances. Thus, when this distance is 1.50 Å at the 2:1 FH:NH$_3$ and 2:1 FH:collidine geometries, $^{1h}J_{H_a-F_a}$ has values of −61 and −57 Hz, respectively, in reasonable agreement with the experimental value of −75 Hz. The negative signs of the computed and experimental coupling constants are indicative of an N−H$_a$−F$_a$ hydrogen bond with little proton-shared character. The values of $^1J_{N-H_a}$ do not vary significantly with geometry and are in reasonable agreement with the experimental value given that the computed $^1J_{N-H_a}$ refers to ammonium instead of collidinium. The remaining coupling constant associated with the N−H$_a$−F$_a$ hydrogen bond decreases dramatically in absolute value as the F$_a$−H$_a$ and therefore the F$_a$−N distances increase, but no experimental value for this coupling constant was reported. However as noted by Limbach,[7] even below 95 K there remains a moderately fast exchange between his equivalent proton-transferred structures 1 and 2, which correspond to the two isomers of our structure 10 with the fluorine atoms exchanged. A reasonable explanation for the absence of an experimental N−F$_a$ coupling constant is not that it does not exist, but that it is smaller than the line width and lost in the broadening caused by the dynamic exchange of the fluorine atoms F$_a$ and F$_b$. In the $^{19}$F signal of F$_a$ at 97 K, only $^{2h}J_{F_a-F_b}$ (155 Hz) is observed, but there is also considerable broadening of this signal that could mask $^{2h}J_{N-F_a}$ as large as 60−70 Hz. Hence, comparisons of $^{2h}J_{N-F_a}$ values are not possible, although it appears that $^{2h}J_{N-F_a}$ has a smaller absolute value in proton-transferred complexes compared to the corresponding equilibrium complexes. With respect to the one- and two-bond coupling constants for the N−H$_a$−F$_a$ hydrogen bond, it makes little difference whether the geometries used for the calculations on the 2:1 FH:NH$_3$ complexes come from optimized 2:1 FH:NH$_3$, 2:1 FH:pyridine, or 2:1 FH:collidine geometries as long as they refer to corresponding proton-transferred structures.

This is not the case for coupling constants involving the F$_b$−H$_b$−F$_a$ hydrogen bond, as is readily apparent from Tables 4 and 7. At the 2:1 FH:collidine geometry, the best agreement between the experimental values of $^{2h}J_{F_b-F_a}$ (155 Hz), $^{1h}J_{H_b-F_a}$ (<10 Hz), and $^1J_{F_b-H_b}$ (280 Hz) is found when the F$_a$−H$_a$ distance is longest and the F$_b$−H$_b$−F$_a$ hydrogen bond has increased proton-shared character. However, the one-bond H$_a$−F$_a$ coupling constant for the N−H$_a$−F$_a$ hydrogen bond is much too small at this distance, and in better agreement with experiment at short F$_a$−H$_a$ distances. This incongruity occurs as a result of taking into account the solvent effect on the N−H$_a$−F$_a$ hydrogen bond by lengthening the F$_a$−H$_a$ distance, but not taking it into account for the F$_b$−H$_b$−F$_a$ hydrogen bond, which has its optimized gas-phase geometry at each distance.

That the solvent might well promote partial proton transfer from F$_b$ to F$_a$ relative to the gas phase can be seen by examining the variation of $^{2h}J_{F_b-F_a}$, $^{1h}J_{H_b-F_a}$, and $^1J_{F_b-H_b}$ at the geometries of the 2:1 FH:NH$_3$ complexes. At distances between 1.50 and 1.70 Å, the changes in all three computed coupling constants sweep through the experimental values. $^{2h}J_{F_b-F_a}$ increases from 95 to 160 Hz (experimental value 155 Hz), $^{1h}J_{H_b-F_a}$ passes through 0 Hz as it changes sign (experimental value <10 Hz), and $^1J_{F_b-H_b}$ decreases from 314 to 184 Hz (experimental value 280 Hz). In these complexes, it is the interaction of F$_b$ with the NH$_4^+$ hydrogens which lengthens the F$_b$−H$_b$ distance and gives increased proton-shared character to the F$_b$−H$_b$−F$_a$ hydrogen bond. Indirectly and fortuitously, this interaction appears to mimic the effect of the solvent and provides information about the F$_b$−H$_b$−F$_a$ hydrogen bond in solution.

In ref 7 N−H$_a$, F$_a$−H$_a$, F$_b$−H$_b$, and H$_b$−F$_a$ distances were estimated from the values of the five spin−spin coupling constants measured experimentally. Another independent approach to investigating spin−spin coupling constants in the proton-transferred 2:1 FH:collidine complex is to optimized the structure of this complex with these distances held fixed and then compute the coupling constants for a 2:1 FH:NH$_3$ complex

**TABLE 9: Structures of Optimized 2:1 FH:Collidine Complexes at Experimental Distances, and Coupling Constants for 2:1 FH:NH$_3$ Complexes at These Geometries**

| | Distances (Å) and Angles (deg) | | | | | | | |
|---|---|---|---|---|---|---|---|---|
| $F_a-H_a$ | $N-H_a$ | $N-F_a$ | $N-H_a-F_a$ | $F_b-H_b$ | $F_a-H_b$ | $F_b-F_a$ | $F_b-H_b-F_a$ | $N-F_a-F_b$ |
| 1.61[a] | 1.05 | 2.648 | 169 | 1.04 | 1.30 | 2.332 | 171 | 99 |
| 1.61[b] | 1.05 | 2.648 | 169 | 1.04 | 1.28 | 2.312 | 169 | 99 |

| | Coupling Constants (Hz) | | | | | |
|---|---|---|---|---|---|---|
| $F_a-H_a$ | $^{1h}J_{F_a-H_a}$ | $^{1}J_{N-H_a}$ | $^{2h}J_{N-F_a}$ | $^{1}J_{F_b-Hb}$ | $^{1h}J_{H_b-F_a}$ | $^{2h}J_{F_b-F_a}$ |
| 1.61[a] | −45.5 | −69.8 | −36.1 | 290.9 | −42.5 | 120.5 |
| 1.61[b] | −45.5 | −69.9 | −36.1 | 286.5 | −38.0 | 141.5 |
| expt[c] | −75 | −86 | ? | 280 | <10 | 155 |

[a] Distances taken from ref 7. [b] Distances from ref 7 but with the $F_a-H_b$ distance shortened to 1.28 Å to give greater proton-shared character to the $F_b-H_b-F_a$ hydrogen bond. [c] Experimental data from ref 7.

at the optimized geometry in the hydrogen bonding region. The optimized structure, the computed coupling constants for this structure, and the experimental coupling constants are given in Table 9. Since the $F_a-H_a$ distance was estimated to be 1.61 Å, it is not surprising that the computed values of $^{1h}J_{F_a-H_a}$, $^{1}J_{N-H_a}$, and $^{2h}J_{N-F_a}$ are very similar to the values computed using the 2:1 FH:collidine geometry with an $F_a-H_a$ distance of 1.60 Å. And, as noted above, it is at the shorter $F_a-H_a$ distances that the coupling constants associated with the $N-F_a-H_a$ hydrogen bond are in better agreement with experiment. Moreover, the shorter $F_b-H_b$ and $F_a-H_b$ distances extracted from the experimental data give the $F_b-H_b-F_a$ hydrogen bond increased proton-shared character and bring the computed values of $^{1h}J_{H_b-F_a}$, $^{1}J_{F_b-H_b}$, and $^{2h}J_{F_b-F_a}$ into better agreement with experiment, although the absolute value of $^{1h}J_{H_b-F_a}$ is still too large, and that of $^{2h}J_{F_b-F_a}$ is too small. This suggests that the $F_b-H_b-F_a$ hydrogen bond still does not have enough proton-shared character. To increase the proton-shared character of this bond, the $H_b-F_a$ distance was shortened from 1.30 to 1.28 Å, and a reoptimized geometry was obtained. At this geometry, both $^{1h}J_{H_b-F_a}$ and $^{2h}J_{F_b-F_a}$ are in better agreement with the experimental values, as can be seen in Table 9. It would be possible to achieve even better agreement with experiment by making relatively small adjustments to bond distances and angles in the $F_b-H_b-F_a$ hydrogen-bonding region, but this would not really lead to a better understanding of these structural and NMR spectroscopic properties. What has already been demonstrated is that a computed structure of a 2:1 FH:collidine complex can describe the hydrogen bonding region well enough to produce computed coupling constants that are in agreement with experimental data. However, for this to occur it is necessary to take into account solvent-induced proton transfer across the $N-H_a-F_a$ hydrogen bond and an increase in the proton-shared character of the $F_b-H_b-F_a$ hydrogen bond due to the presence of solvent. The geometry of an optimized 2:1 FH:collidine complex with experimental $F_a-H_a$, $N-H_a$, $F_b-H_b$, and $H_b-F_a$ distances produces computed coupling constants that are in good agreement with experimental data.

## Conclusions

This paper reports the results of an ab initio investigation of a variety of 2:1 FH:NH$_3$ complexes (F$_b$H$_b$:F$_a$H$_a$:NH$_3$) and the effect of geometry changes in these complexes on one- and two-bond spin−spin coupling constants across $F_a-H_a-N$ and $F_b-H_b-F_a$ hydrogen bonds. The data obtained have also been used to provide insight into spin−spin coupling constants measured experimentally for 2:1 FH:collidine complexes. The results of this study support the following statements.

1. The equilibrium structure of the 2:1 FH:NH$_3$ complex is stabilized by a traditional $F_a-H_a-N$ hydrogen bond which has significant proton-shared character. Along the proton-transfer coordinate as H$_a$ is transferred to N, $^{2h}J_{F_a-N}$ exhibits its maximum absolute value for a quasi-symmetric proton-shared hydrogen bond, $^{1}J_{F_a-H_a}$ decreases, and the absolute value of $^{1h}J_{H_a-N}$ increases. After H$_a$ is transferred to N, H$_b$ is transferred from F$_b$ to F$_a$, and subsequently the in-plane H of NH$_3$ is transferred to F$_b$. Along this pathway there exists a transition structure in which NH$_4^+$ is a double proton donor to FHF$^-$. The final structure is equivalent to the original with F$_a$ and F$_b$ interchanged.

2. While one- and two-bond spin−spin coupling constants associated with the $F_a-H_a-N$ hydrogen bond exhibit expected behavior as the $F_a-N$ and $F_a-H_a$ distances change, such is not the case for coupling constants associated with the $F_b-H_b-F_a$ hydrogen bond, particularly $^{2h}J_{F_b-F_a}$. $^{2h}J_{F_b-F_a}$ is strongly dependent on the F−F distance and the orientation of the hydrogen-bonded species. Moreover, $^{2h}J_{F_b-F_a}$ receives large contributions of opposite signs from the PSO and FC terms, making it difficult to predict the value of $^{2h}J_{F_b-F_a}$ in any particular complex.

3. The structures of perpendicular proton-transferred complexes have $N-F_a$ and $F_a-H_a$ coupling constants that are small owing to long distances and nonlinearity of the $N-H_a-F$ hydrogen bonds, and F−F and $F-H_b$ coupling constants that do not agree with experimental values. Such complexes are most probably not responsible for the experimentally measured coupling constants of 2:1 FH:collidine complexes in solution.

4. Relatively small geometry changes in the hydrogen-bonding region can have large effects on coupling constants, particularly those associated with the $F_b-H_b-F_a$ hydrogen bond.

5. Replacing the collidine N by the N of ammonia changes $N-F_a$ and N−H coupling constants. However, the changes observed are those anticipated from previous theoretical and experimental studies of N−F and N−H coupling involving these two types of N atoms.

6. $N-F_a$, $F_a-H_a$, and $N-H_a$ coupling constants computed for 2:1 FH:NH$_3$ complexes are in better agreement with experiment when the $F_a-H_a$ distance is short, irrespective of whether the geometry is taken from optimized proton-tranferred 2:1 FH:NH$_3$, 2:1 FH:pyridine, or 2:1 FH:collidine geometries. However, better agreement between computed and experimental $F_b-F_a$, $F_b-H_b$, and $H_b-F_a$ coupling constants is found for complexes with longer $F_a-H_a$ distances.

7. The best agreement between computed and experimental $F_b-F_a$, $F_b-H_b$, and $H_b-F_a$ coupling constants is found for the 2:1 FH:NH$_3$ geometries, when F$_b$ interacts with the ammonium hydrogens. This interaction appears to mimic interaction with

the solvent. To obtain agreement between computed and experimental data, account must be taken of the role of the solvent in promoting proton transfer across both $F_a-H_a-N$ and $F_b-H_b-F_a$ hydrogen bonds.

**Acknowledgment.** This work was supported by a grant from the U.S. National Science Foundation (NSF CHE-9873815) and by the Spanish DGI/MCyT (Project No. BQU-2003-01251). The authors gratefully acknowledge this support and that of the Ohio Supercomputer Center. Helpful suggestions given by Professor H.-H. Limbach are greatly appreciated by the authors.

## References and Notes

(1) Del Bene, J. E.; Bartlett, R. J.; Elguero, J. *Magn. Reson. Chem*. **2002**, *40*, 767.

(2) Shenderovich, I. G.; Burtsev, A. P.; Denisov, G. S.; Golubev, N. S.; Limbach, H−H. *Magn. Reson. Chem*. **2001**, *39*, S91.

(3) Golubev, N. S.; Shenderovich, I. G.; Smirnov, S. N.; Denisov, G. S.; Limbach, H−H. *Chem. Eur. J*. **1999**, *5*, 492.

(4) Del Bene, J. E.; Elguero, J. *Magn. Reson. Chem*. **2004**, *42*, 421.

(5) Del Bene, J. E.; Elguero, J. *J. Am. Chem. Soc*. **2004**, *126*, 15624.

(6) Del Bene, J. E.; Elguero, J. *J. Phys. Chem. A* **2004**, *108*, 11762.

(7) Shenderovich, I. G.; Tolstoy, P. M.; Golubev, N. S.; Smimov, S. N.; Denisov, G. S.; Limbach, H−H. *J. Am. Chem. Soc*. **2003**, *125*, 11710.

(8) Del Bene, J. E.; Elguero, J.; Alkorta, I.; Mó, O.; Yañez, M. *J. Phys. Chem. A* **2005**, *109*, 2350.

(9) Pople, J. A.; Binkley, J. S.; Seeger, R. *Int. J. Quantum Chem., Quantum Chem. Symp*. **1976**, *10*, 1.

(10) Krishnan, R.; Pople, J. A. *Int. J. Quantum Chem*. **1978**, *14*, 91.

(11) Bartlett, R. J.; Silver, D. M. *J. Chem. Phys*. **1975**, *62*, 3258.

(12) Bartlett, R. J.; Purvis, G. D. *Int. J. Quantum Chem*. **1978**, *14*, 561.

(13) Hehre, W. J.; Ditchfield, R.; Pople, J. A. *J. Chem. Phys*. **1982**, *56*, 2257.

(14) Hariharan, P. C.; Pople, J. A. *Theor. Chim. Acta* **1973**, *238*, 213.

(15) Spitznagel, G. W.; Clark, T.; Chandrasekhar, J.; Schleyer, P. v. R. *J. Comput. Chem*. **1982**, *3*, 3633.

(16) Clark, T.; Chandrasekhar, J.; Spitznagel, G. W.; Schleyer, P. v. R. *J. Comput. Chem*. **1983**, *4*, 294.

(17) Perera, S. A.; Sekino, H.; Bartlett, R. J. *J. Chem. Phys*. **1994**, *101*, 2186.

(18) Perera, S. A.; Nooijen M.; Bartlett, R. J. *J. Chem. Phys*. **1996**, *104*, 3290.

(19) Perera, S. A.; Bartlett, R. J. *J. Am. Chem. Soc*. **1995**, *117*, 8476.

(20) Perera, S. A.; Bartlett, R. J. *J. Am. Chem. Soc*. **1996**, *118*, 7849.

(21) Schäfer, A.; Horn, H.; Ahlrichs, R. *J. Chem. Phys*. **1992**, *97*, 2571.

(22) Dunning, T. H., Jr. *J. Chem. Phys*. **1989**, *90*, 1007.

(23) Woon DE.; Dunning, T. H., Jr. *J. Chem. Phys*. **1995**, *103*, 4572.

(24) Kirpekar, S.; Jensen, H. J. Aa.; Oddershede, J. *Chem. Phys*. **1994**, *188*, 171.

(25) Del Bene, J. E.; Jordan MJT.; Perera, S. A.; Bartlett, R. J. *J. Phys. Chem. A* **2001**, *105*, 8399.

(26) Del Bene, J. E.; Perera, S. A.; Bartlett, R. J. *Magn. Reson. Chem*. **2001**, *39*, S109.

(27) Del Bene, J. E.; Perera, S. A.; Bartlett, R. J.; Elguero, J.; Alkorta, I.; López-Leonardo, C.; Alajarin, M. *J. Am. Chem. Soc*. **2002**, *124*, 6393.

(28) Del Bene, J. E.; Elguero, J.; Alkorta, I. *Z. Phys. Chem*. **2003**, *217*, 1565.

(29) Del Bene, J. E.; Elguero, J.; Alkorta, I. *J. Phys. Chem. A* **2004**, *108*, 3662.

(30) Frisch, M. J.; Trucks, G. W.; Schlegel, H. B.; Scuseria, G. E.; Robb, M. A.; Cheeseman, J. R.; Montgomery, J. A., Jr.; Vreven, T.; Kudin, K. N.; Burant, J. C.; Millam, J. M.; Iyengar, S. S.; Tomasi, J.; Barone, V.; Mennucci, B.; Cossi, M.; Scalmani, G.; Rega, N.; Petersson, G. A.; Nakatsuji, H.; Hada, M.; Ehara, M.; Toyota, K.; Fukuda, R.; Hasegawa, J.; Ishida, M.; Nakajima, T.; Honda, Y.; Kitao, O.; Nakai, H.; Klene, M.; Li, X.; Knox, J. E.; Hratchian, H. P.; Cross, J. B.; Bakken, V.; Adamo, C.; Jaramillo, J.; Gomperts, R.; Stratmann, R. E.; Yazyev, O.; Austin, A. J.; Cammi, R.; Pomelli, C.; Ochterski, J. W.; Ayala, P. Y.; Morokuma, K.; Voth, G. A.; Salvador, P.; Dannenberg, J. J.; Zakrzewski, V. G.; Dapprich, S.; Daniels, A. D.; Strain, M. C.; Farkas, O.; Malick, D. K.; Rabuck, A. D.; Raghavachari, K.; Foresman, J. B.; Ortiz, J. V.; Cui, Q.; Baboul, A. G.; Clifford, S.; Cioslowski, J.; Stefanov, B. B.; Liu, G.; Liashenko, A.; Piskorz, P.; Komaromi, I.; Martin, R. L.; Fox, D. J.; Keith, T.; Al-Laham, M. A.; Peng, C. Y.; Nanayakkara, A.; Challacombe, M.; Gill, P. M. W.; Johnson, B.; Chen, W.; Wong, M. W.; Gonzalez, C.; Pople, J. A. *Gaussian 03*, revision C.02; Gaussian, Inc.: Wallingford, CT, 2004.

(31) Stanton, J. F.; Gauss, J.; Watts, J. D.; Nooijen, M.; Oliphant, N.; Perera, S. A.; Szalay, P. G.; Lauderdale, W. J.; Gwaltney, S. R.; Beck, S.; Balkova, A.; Bernholdt, D. E.; Baeck. K.-K.; Tozyczko, P.; Sekino, H.; Huber, C.; Bartlett, R. J. *ACES II*, a program product of the Quantum Theory Project; University of Florida: Gainesville, FL. Integral packages included are as follows: VMOL (Almlöf, J.; Taylor, P. R.); VPROPS (Taylor, P. R.); ABACUS (Helgaker, T.; Jensen, H. J. Aa.; Jørgensen, P.; Olsen, J.; Taylor, P. R.). Brillouin-Wigner perturbation theory was implemented by J. Pittner.

(32) Del Bene, J. E.; Elguero, J.; Alkorta, I.; Yañez, M.; Mó, O. *J. Chem. Phys*. **2004**, *120*, 3237.

(33) Ramos M.; Alkorta, I.; Elguero, J.; Golubev, N. S.; Denisov, G. S.; Benedict, H.; Limbach, H−H. *J. Phys. Chem. A* **1997**, *101*, 9791.

(34) Del Bene, J. E.; Perera, SA.; Barltett, R. J.; Yañez, M.; Mó, O.; Elguero, J.; Alkorta, I. *J. Phys. Chem. A* **2003**, *107*, 3121.

(35) Del Bene, J. E.; Perera, SA.; Barltett RJ.; Yañez, M.; Mó, O.; Elguero, J.; Alkorta, I. *J. Phys. Chem. A* **2003**, *107*, 3126.

(36) Del Bene, J. E. In *The Electronic Encyclopedia of Computational Chemistry*; Schleyer, P. v. R., Allinger, N. L., Clark, T., Gasteiger, J,, Schaefer, H. F., III, Schreiner, P. R., Eds.; John Wiley & Sons: Chichester, U.K., 2004.

(37) Berger, S.; Braun, S.; Kalinowski, H.-O. *NMR Spectroscopy of the Nonmetallic Elements*; John Wiley & Sons: Chichester, U.K., 1997; pp 245−247.